Dynamic Processes Modeling in a Peristaltic Pump with a Hydraulic Drive for the Bingham Fluid

Vladimir Shatokhin [1], Yaroslav Ivanchuk [2], Olha Dvirna[3*],
Natalia Veselovskaya[4], Wojciech Jurczak [5]

[1] Department of Building and Theoretical Mechanics, Kharkiv National University of Civil Engineering and Architecture, 40, Sumska St., 61002, Kharkiv, Ukraine

[2] Department of Computer Science, Vinnytsia National Technical University, 95, Khmel'nyts'ke Ave., 21021, Vinnytsia, Ukraine

[3] Department of Engineering Sciences, Faculty of Marine Engineering, Gdynia Maritime University, 81-87 Morska St., 81-225 Gdynia, Poland

[4] Department of Machinery and Equipment of Agricultural Industry, Vinnytsia National Agrarian University, 3, Sonyachna St., 21008, Vinnytsia, Ukraine

[5] Department of Mechanical-Electrical Engineering, Polish Naval Academy, 69, Śmidowicza St., 81-127, Gdynia, Poland

* Corresponding author's email: o.dvirna@wm.umg.edu.pl

ABSTRACT

At present peristaltic pumps are widely used in many branches of industry and national economy. Simplicity of construction, processability and possibility of pumping liquids with big quantity of solid particles are the main advantages while using peristaltic pumps. Therefore development of methods of rational choice of parameters at designing of peristaltic pumps is the actual problem. To develop universal mathematical models of dynamic processes in peristaltic pumps for definition of rational technical parameters. In dynamic processes we propose to use differential equations of motion in the Lagrange form, where the angle of rotation of the pump rotor is taken as a universal coordinate. Mathematical model of dynamic processes in peristaltic pump with hydraulic drive has been created on the base of differential equation. The function of resistance forces caused by gravity forces of mixture particles in the hose reel has been determined. On the basis of the non-linear model of the resistance forces to the flow of the fluid Bingham method of constructing the dependence of the pressure drop on the angular velocity of the rotor to determine the resistance forces to the flow of the fluid has been proposed. The result of dynamic processes simulation is the determination of interrelationship of technological parameters of the device functioning: the velocity of the medium and pump performance is increasing at reducing the length of the diverting hose and reducing the height of its rise; a significant influence on the average speed has plastic viscosity of the environment; a significant change in the yield strength has an insignificant impact on the speed.

Keywords: peristaltic pump, dynamic process simulation, the Bingham fluid, hydraulic drive, pump rotor

INTRODUCTION

Peristaltic pumps have a number of important advantages: simple design, tight seal, self-suction, ease of delivery rate control of the mixture, and the ability of liquids transmission with a large number of solids. The devices are widely used in the mining and concentrating industry, construction, chemical, and food production, woodworking, and pulp, and paper industries, etc.

The creation of peristaltic pumps and methods of the rational choice of their parameters is a vital task. One of the up-to-date efficient ways of its solution is the adequate modeling of dynamic processes in these mechanisms. Currently, the efforts of researchers are concentrated on solving

individual tasks associated with the creation of new models of devices. These include, in particular, the tasks of a hydraulic control system modeling and a high-torque hydraulic motor; assessment of power consumption for the process of the mixture transportation and the discharge pressure that the pump must create; assessment of the mixture uneven supply and the mixture motion speed at the outlet of the pipeline, etc.

Currently, there is a fairly large number of literature sources providing details of peristaltic pumps, which consider the design of pumps, their characteristics, and fields of application [1, 2]. At the same time, there are a limited number of studies devoted to the calculating theory of this type of pumps, dynamic processes modeling in them.

In work [3], the technological capabilities of the pump are being considered, in work [4], its hydraulic characteristics and the robot of the pressing rollers are being analyzed. Studies of the issue of the flow pulsations reducing of the mixture which is pumped were considered in [1].

In work [3], the technological capabilities of the pump are being considered, in work [4], its hydraulic characteristics and the robot of the pressing rollers are being analyzed. Studies of the issue of the flow pulsations reducing of the mixture which is pumped have been considered in work [1]. One of the ways to reduce the pulsations can be the use of classical management methodology with a feedback mechanism [5]. In this case, however, a level decrease of pulsations leads to an increase in the injection pressure of the solution.

Otherwise, the level of pulsations can be reduced by increasing the number of pressure rollers of the pump, however, this reduces the service life of the working part of the hose in the pump housing [6].

The matter of fluid flow pulsation and optimization of its parameters are studied in work [7]. The properties of the test medium, however, differ significantly from the properties of the mixture flow, which is being pumped by a hose concrete pump.

At the present, there are no models of dynamic processes that would reflect the causes of the emergence of pulsations and make it possible to assess the irregularity degree of the mixture supply by a peristaltic pump to pipelines.

In the article [8], an axial piston motor is considered as a drive. A detailed mathematical model of the hydraulic system is presented, in which the

pump is put into action by an axial piston pump, but the model does not take into account the effect of the mixture moving in the pipeline.

A mathematical model of a modern portable concrete pump is presented in work [9], but in the capacity of an executing mechanism in the given device a hydraulic cylinder is used.

A number of literature sources contain details about piston less peristaltic pumps [10, 11], where pump designs, their characteristics and fields of application are being considered. At the same time, questions dedicated to their origin, as well as calculating theory of pumps of this type, are presented very limitedly.

A mathematical model of dynamic processes in a peristaltic pump with a hydraulic drive is created in work [12], in which the moving mixture is considered as Newtonian fluid. In many cases, however, mixtures are non-Newtonian fluids, in particular, Bingham plastic fluids [13–15]. In them, the shear velocity at each point represents some stress function at that point. The concept of an idealized Bingham fluid is convenient for practice, as a lot of real liquid mixtures are very close to this type: construction mixes, concrete mixtures, bitumen (in a certain temperature range), drilling fluids, oil paints, etc. Works [16–17] are dedicated to the flow researches of rheologically complex mediums.

The basic apparatus of mathematical modelling of dynamic processes in the actuator based on axial piston hydraulic motors are precise methods of non-linear mechanics, which are based on fitting solutions [18], describing adjacent intervals of actuator motion. These methods have made it possible to study in detail the complex dynamic process of a number of peristaltic pumping machines motions and to reveal their fundamental properties. However, the use of these methods to build mathematical models of a wide range of pumping systems based on a hydraulic drive is labor-intensive and limited in their area of application, especially when the dimensionality of the systems increases, as well as the need to account for additional non-linear factors and the complexity of the nature of perturbations from the action of non-periodic and random forces.

A generally recognized approach to modeling of fluid pulsations in pumping systems is the method of asymptotic representation of solutions in powers of small parameter [19] in the analysis of basic harmonic components of oscillations. It is based on the derivation of more usual relations

from their general mathematical description passing to spectral representations [17] and ideas of the equivalent linearization [20], but it does not allow finding an acceptable mathematical model for the vibration systems. This leads to necessity of development of new methods and approaches for development of the reference mathematical models of fluid motion dynamics for a wide range of peristaltic pumping systems.

The physical parameters of the energy carrier (working fluid) and design parameters of hydraulic drive [15], providing control of pump operation, have a great influence on increasing of speed, power capacity and compactness of peristaltic pumping machines. It leads to development of mathematical models in the form of systems of differential equations of motion of the hydraulic drive structural elements [21] on the basis of the synthetic dynamic model with the reduced coefficients for the oscillating system. Practical realization of the given approach is possible only for mathematical models mainly of low dimensionality, and describes properties of objects in a narrow range of such working parameters change.

Experience shows that in order to overcome the above difficulties, it is necessary to set a new problem of mathematical modelling of irregular mixture feeding process and mixture velocity at the pipeline exit in spatially unsteady form, requiring development of new more complete and adequate mathematical models based on the system of Lagrange differential equations of the second kind and non-linear model of resistance forces to mixture movement, being Bingham environment, obtained through Buckingham equation [10]. The question about the possibility of replacing the physical experiment with a numerical one using computer simulation methods remains relevant.

The article covers the presentation of the research results on the creation of more advanced models of dynamic processes in peristaltic pumps, taking into account the fact that mixtures in many cases represent a Bingham medium [22] .

The purpose of the work is the creation of universal mathematical models of dynamic processes in peristaltic pumps with a hydraulic drive to determine the technological qualities of devices, the choice of rational parameters. The models should contain the main parameters of pumps, drives, hoses, transferrable mixtures, which is due to the needs to modernize existing models and develop new models of peristaltic pumps [23, 24].

The models should contain the main parameters of pumps, drives, hoses, transferable mixtures, which is due to the needs to modernize existing models and develop new models of peristaltic pumps.

In the furtherance of this goal, the following tasks must be solved: there was developed a method for forming the resisting moment on the pump rotor from the rollers that deform the hose; models were produced of friction forces that prevent the movement of the mixture through the hose; an equation was obtained for the resistance forces conditioned by the gravitational forces of the mixture particles during its rise; a model of the hydraulic motor torque as an angular rate function of its rotor was built with the use of the catalog data; calculation studies of the consistent patterns of dynamic processes in the pump were conducted with the help of the developed versatile models.

As a research method for dynamic processes, it was suggested to use differential equations of motion written in the Lagrange form, at the construction of which the rotation angle of the pump rotor is taken as a generalized coordinate. For calculation studies, the mathematical package MathCAD was applied.

MATHEMATICAL MODEL

The calculation model of the peristaltic pump is shown in Figure 1. Used symbols: d – a diameter of a hose (internal); h – a hose wall thickness; D – a hose diameter (outer); R – a radius of the pump housing along the inner wall; R_1 – a radius equal to the distance between the centers of the rotor and the central roller; R_2 – a radius is equal to the distance between the centers of the rotor and the side roller; R_C – a radius of the axis of the hose bent part; d_0 – a diameter of central and side rollers; α – an angle between central and side rollers; φ – the direction of the angle reading that determines the position of the rotor (which is counted from the vertical counterclockwise).

Building a dynamic model of the pump rotor requires the establishment of the dependencies of the force moments; applied to the rotor on its angle of rotation. To form the moment of resistance forces from rolling the rollers along the hose, it is necessary to position angles that form segments connecting the mass centers of the roller and the rotor at the moment of the roller contact with the hose (Figure 2).
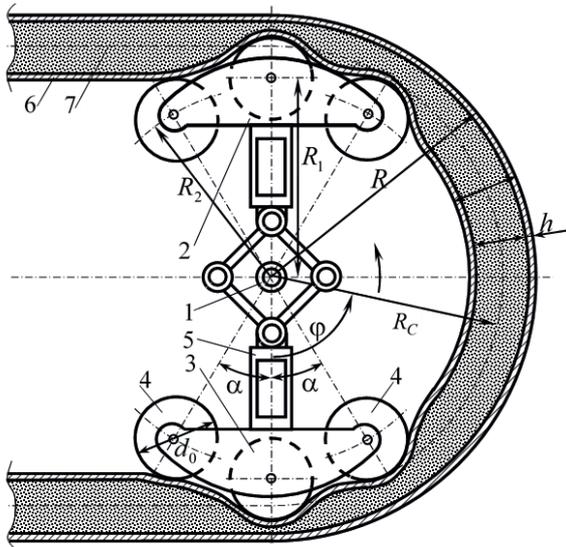
Fig. 1. The calculation model of the peristaltic pump: 1 – pump shaft; 2 – frame; 3 – central (pressure) roller; 4 – side (pinch) roller; 5 – appliance for changing the surface contact radius of rollers with a hose 6; 7 – fluid medium; arc arrow indicates the direction of rotor rotation.

With the help of the indicated scheme and obvious geometric relationships, we have for the angles:

$$\beta_i = \arcsin\frac{R - D - \dfrac{d_0}{2}}{R_i} \qquad (1)$$

$$\alpha_i = \frac{\pi}{2} - \beta_i \quad (i = 1,2)$$

In these formulas, the index $i = 1$ corresponds to the central roller, $i = 2$ – to the side one. Please note that the same by the module will be the angles corresponding to the contact loss torque between the rollers and the hose.

The above considerations allow us to assert that the process of changing the resistance moment, which prevents the roller from rolling, when the rotor turns, includes three stages: an escalation in the hose deformation from the roller rolling; displacement of the solution at the maximum hose deformation; reduction of the hose deformation when the roller "exits" contact with the hose.

For the preservation of the traditional form of representation of the maximum moment of resistance forces:

$$M_{\text{тр}} = N f_k \qquad (2)$$
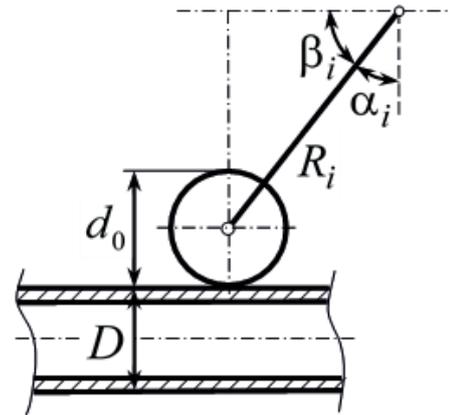
**Fig. 2.** A scheme to determine the angles of the roller contact with the hose

it appeared to be viable to attribute these three stages during the model development to the nature of the change of the rolling friction coefficient f_k, and the normal component of the hose reaction (normal pressure force) N was accepted as constant. The dependence diagram of the friction coefficient for the central roller is shown in Figure 3, when its maximum value is $\delta_1 = 2$ cm.

Similar diagrams for the left and right side rollers are shown in Figures 4, 5 when the maximum friction coefficient is $\delta_2 = 1$ cm.

If we do not take into account the displacement relative to the horizontal axis, the qualitative character of the change in the friction coefficient in all three diagrams is the same. The
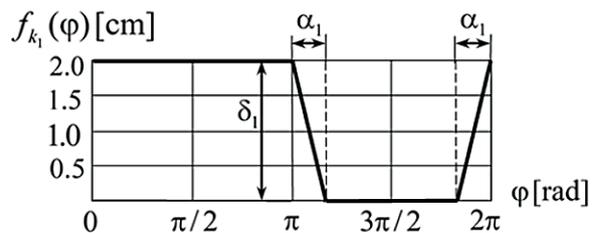
Fig. 3. Dependency of the rolling friction coefficient of central roller from a roller turning angle
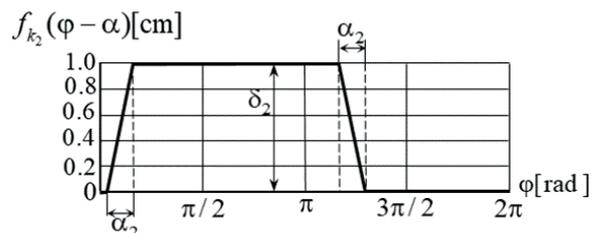
Fig. 4. Dependency of the rolling friction coefficient of left roller from a roller turning angle
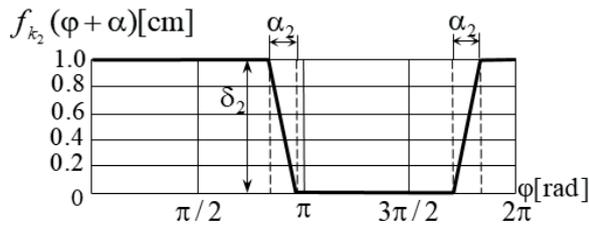
Fig. 5. Dependency of the rolling friction coefficient of side roller from a roller turning angle

displacements due to the fact that the left side roller "gets behind" the central one by an angle α, and the right one, respectively, "gets ahead" by an angle α. These piecewise linear functions are described analytically by the expression:

$$f_{k_i}(\varphi) = \begin{cases} \delta_i, & \varphi \le \pi; \\ \delta_i\left(\dfrac{\pi - \varphi}{\alpha_i} + 1\right), & \pi < \varphi < \pi + \alpha_i; \\ 0, & \pi + \alpha_i \le \varphi \le 2\pi - \alpha_i; \\ \delta_i\left(\dfrac{\varphi - 2\pi}{\alpha_i} + 1\right), & 2\pi - \alpha_i < \varphi \le 2\pi \quad (i = 1,2). \end{cases} \quad (3)$$

The laws of change in the coefficient of rolling friction on the intervals of implementation and exit of the roller from contact with the deformed hose are assumed to be linear. This does not reduce the similarity of the proposed model: firstly, these intervals make up an insignificant fraction of the rotor complete rotation, so the effect of taking into account the nonlinear nature of this dependence will be insignificant; secondly, taking into account such a dependence, for example, obtained by calculation or experimentally, at software implementation of algorithms does not present any difficulties. In Figure 6 is an auxiliary diagram explaining the conversion of the rolling resistance moment of the central roller $M_{тр1}$ to the rotor rotation resistance moment M.

In Figure 6: T_1 – the driving force applied to the axis of the roller; T_1' – the force applied to the rotor (the modules of these forces are the same $T_1' = T_1$); G_1 – roller pressing force; N_1, $F_{тр1}$ – respectively, the normal reaction of the hose and the friction force acting from the side of the hose on the roller.

For the force applied to the rotor, taking into account (3), we have:

$$T_1(\varphi) = \frac{M_{тр_1}(\varphi)}{\dfrac{d_0}{2}} = \frac{G_1 \cdot f_{k_1}(\varphi)}{\dfrac{d_0}{2}} \quad (4)$$

$$M(\varphi) = T_1'(\varphi) \cdot R_1 = T_1(\varphi) \cdot R_1 \quad (5)$$

Now the total moment of resistance on the rotor from the three rollers of the lower cage is based on formulas (3) – (5) (see Figure 1):

$$M_1(\varphi) = \frac{G_1 \cdot f_{k_1}(\varphi)}{\dfrac{d_0}{2}} \cdot R_1 + \frac{G_2 \cdot f_{k_2}(\varphi - \alpha)}{\dfrac{d_0}{2}} \cdot$$
$$\cdot R_2 + \frac{G_2 \cdot f_{k_2}(\varphi + \alpha)}{\dfrac{d_0}{2}} \cdot R_2 \quad (6)$$

The two latter terms in formula (6) correspond to the resistance moment from the left and right side rollers. The expression of the resistance moment from the rollers of the upper "leading" frame will differ from (6) increased on π by the value of an argument:

$$M_2(\varphi) = M_1(\varphi + \pi) \quad (7)$$

Then the total resistance moment on the rotor from the rollers rolling will be:

$$M_k(\varphi) = M_1(\varphi) + M_2(\varphi) \quad (8)$$

In Figure 7 are displayed diagrams of the total resistance moment and its components, when $G_1 = 100$ N, $G_2 = 50$ N. The technological characteristics of the pump are significantly affected by the forces of resistance to the mixture movement in the hose. In the case of a Newtonian fluid,
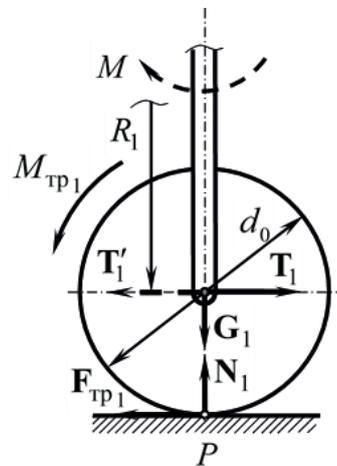
Fig. 6. The resistance moment on rotor at rolling roller

these forces were obtained in [12] with the use of the head (pressure) loss formula at a laminar fluid flow in a round pipe of length *l*. The creation of more perfect models of dynamic processes in these devices requires taking into account the fact that in many cases mixtures are non-Newtonian fluids, in particular, Bingham plastic fluids. For them, the resistance forces obtain a non-linear character. This can be reached in the following way as shown in Figure 8.

It is known that for a laminar flow of a Newtonian fluid [13]:

$$\tau = -\mu \frac{du}{dr} \qquad (9)$$

where: τ – the tangential shear stress displacement at the radius r;

μ – dynamic coefficient of viscosity;

$\frac{du}{dr}$ – the derivative of the velocity in the direction of the radius (the shear rate of neighboring layers of the liquid – with increase r speed decreases).

Points 1, 2 lie on a straight line perpendicular to the velocity. Over time Δt, the points will shift by Δx_1 and Δx_2, respectively. The shift

will be: $\Delta \gamma = \dfrac{\Delta x_2 - \Delta x_1}{\Delta r}$. Diving both parts on

Δt, will get: $\dfrac{\Delta \gamma}{\Delta t} = \dfrac{\dfrac{\Delta x_2}{\Delta t} - \dfrac{\Delta x_1}{\Delta t}}{\Delta r}$.

Since the flow velocities at two points that lie at a distance Δr are equal to $\dfrac{\Delta x_1}{\Delta t} = u_1$ and $\dfrac{\Delta x_2}{\Delta t} = u_2$, passing to the limit, we have:

$$\frac{d\gamma}{dt} = -\frac{du}{dr} \qquad (10)$$

The minus sign in formula (10) is due to the fact that with increasing r the speed decreases $\frac{du}{dr} < 0$. If we consider the direction counter clockwise to be the positive reference direction of the angle γ (see Figure 8), then we indeed arrive at formula (10). Taking into account (10), formula (9) takes the form:

$$\dot{\gamma} = \frac{\tau}{\mu} \qquad (11)$$

If the fluid properties do not depend on time, then the rheological equation which connects the shear stress and shear rate, in the general case,
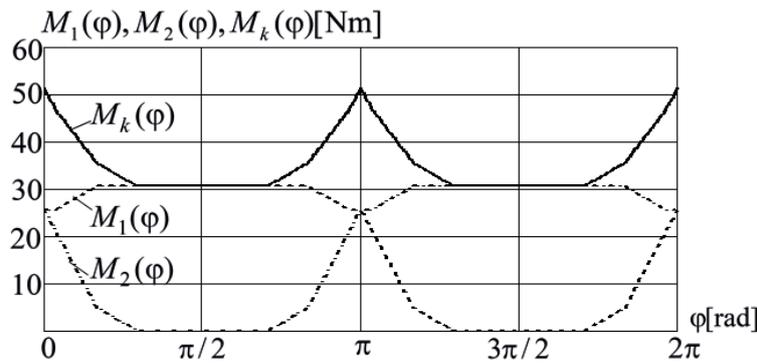

Fig. 7. The total resistance moment on the rotor $M_k(\varphi)$, $M_1(\varphi)$, $M_2(\varphi)$ – resistance moments from the bottom and upper frame
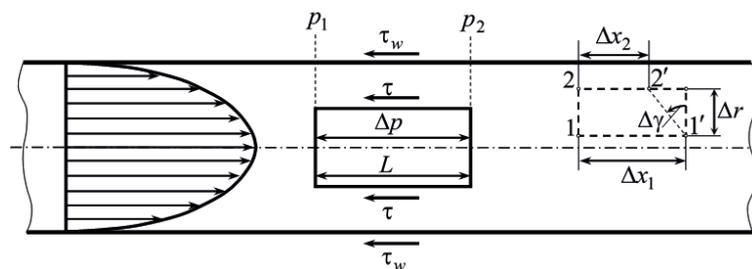

Fig. 8. Building shear velocity dependence on friction stress

is written as [13]: $\dot{\gamma} = f(\tau)$. For the flow in the pipe, taking into account (10), we have:

$$-\frac{du}{dr} = f(\tau) \tag{12}$$

The equilibrium condition of forces which acts on a cylindrical fluid element of radius r and dyne L (see Figure 8) determines the expression:

$$2\pi r L \tau = \pi r^2 \Delta p, \tag{13}$$

where: $\Delta p = p_2 - p_1$ – differential pressure.

From the last expression, it follows:

$$\tau = \frac{r\Delta p}{2L} \tag{14}$$

For the friction stress on the wall, we obtain:

$$\tau_w = \frac{R\Delta p}{2L} \tag{15}$$

Therefore:

$$\tau = \tau_w \frac{r}{R}. \tag{16}$$

and formula (12) is written as:

$$-\frac{du}{dr} = f\left(\tau_w \frac{r}{R}\right) \tag{17}$$

Integration gives:

$$-\int_{u(r)}^{u(R)} du = \int_r^R f\left(\tau_w \frac{r}{R}\right) \tag{18}$$

By assuming the validity of the adhesion conditions of the liquid on the wall (nonslip) $u(R) = 0$, then from the last expression, it follows:

$$u(r) = \int_r^R f\left(\tau_w \frac{r}{R}\right) \tag{19}$$

For the expense we now have:

$$Q = \int_0^R 2\pi r u(r) dr \tag{20}$$

or

$$Q = \pi \int_0^R u(r) d(r^2) \tag{21}$$

Since $u(R) = 0$, and based on (19), $du(r) = -f\left(\tau_w \frac{r}{R}\right)$ then integration by parts gives:

$$Q = \pi \int_0^R r^2 f\left(\tau_w \frac{r}{R}\right) dr \tag{22}$$

Substituting from (16) $r = R\dfrac{\tau}{\tau_w}$, we get:

$$Q = \pi \frac{R^3}{\tau_w^3} \int_0^{\tau_w} \tau^2 f(\tau) d\tau \tag{23}$$

In the case of a Newtonian fluid for laminar flow, on the ground of (11):

$$f(\tau) = \frac{\tau}{\mu} \tag{24}$$

Substituting from (23), we get:

$$Q = \pi \frac{R^3}{\mu \tau_w^3} \int_0^{\tau_w} \tau^3 d\tau \tag{25}$$

and after integrating:

$$Q = \frac{\pi R^3 \tau_w}{4\mu} \tag{26}$$

Substitution τ_w from (16) leads to the well-known Poiseuille equation for the laminar flow of a Newtonian fluid:

$$Q = \frac{\pi R^4 \Delta p}{8\mu L} \tag{27}$$

The flow curve for Bingham fluids is a straight line that intersects the shear stress axis at a distance τ_y from its origin as shown in Figure 9.

The yield stress τ_y is the limit, the excess of which leads to the appearance of a viscous flow. The rheological equation for Bingham plastics can be written as:

$$\dot{\gamma} = \frac{\tau - \tau_y}{\mu_p} = f(\tau), \ (\tau > \tau_y) \tag{28}$$

where: μ_p– plastic viscosity or stiffness coefficient in shear;

$f(\tau)$ – discontinuous function:

$$f(\tau) = \begin{cases} 0, & 0 \leq \tau \leq \tau_y \\ \dfrac{\tau - \tau_y}{\mu_p}, & \tau_y < \tau \leq \tau_w \end{cases} \tag{29}$$

When flowing in a pipe, the friction stresses drop to zero on the axis, and in the near-axial region, where the shear stresses are below the yield strength τ_y, the material does not undergo shear, moving along the axis like a solid rod. The Bingham fluid flow diagram is shown in Figure 10.

Substituting the expression $f(\tau)$ from (29) into formula (23) gives:

$$Q = \frac{\pi R^3}{\mu_p \tau_w^3} \int_{\tau_y}^{\tau_w} \tau^2 (\tau - \tau_y) d\tau \tag{30}$$

By performing the integration, we find:

$$Q = \frac{\pi R^3 \tau_w}{\mu_p} \left[\frac{1}{4} - \frac{1}{3}\left(\frac{\tau_y}{\tau_w}\right) + \frac{1}{12}\left(\frac{\tau_y}{\tau_w}\right)^4 \right] \tag{31}$$

Substituting into (31) the expression for τ_w from (16), we result in the relation known as the Buckingham equation:

$$Q(\Delta p) = \frac{\pi R^4 \Delta p}{8 L \mu_p} \left[1 - \frac{4}{3}\left(\frac{2 L \tau_y}{R \Delta p}\right) + \frac{1}{3}\left(\frac{2 L \tau_y}{R \Delta p}\right)^4 \right] \tag{32}$$

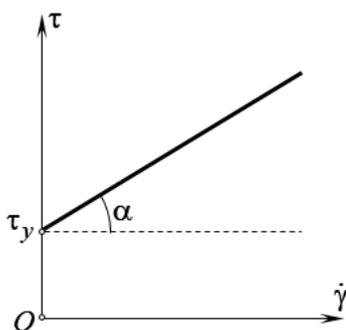When the yield strength τ_y is zero, expression (32) coincides with the Poiseuille formula (27).

Formula (32) can be applied if $\tau_y < \tau_w = \dfrac{R \Delta p}{2L}$. Then the movement of the medium will be possible at $\Delta p > \dfrac{2 L \tau_y}{R}$.

Therefore, the ultimate minimum value of the differential pressure:

$$\Delta p_{min} = \frac{2 L \tau_y}{R} \tag{33}$$

there is no movement of the medium, consumption $Q(\Delta p_{min}) = 0$.

Now for the medium average velocity, we have, taking into account (32):

$$v_{cp} = \frac{Q(\Delta p)}{\pi R^2} \tag{34}$$

On the other hand, for the considered construction of the peristaltic pump, as the average speed, it is feasible to take the expression:

$$v_{cp} = \left(R_1 + \frac{d_0}{2} \right) \dot{\varphi}, \tag{35}$$

where: $\dot{\varphi}$ – pump rotor angular velocity.

Comparison of the right parts of formulas (34) and (35) allows us to write an expression for the angular velocity of the pump rotor:

$$\dot{\varphi} = \frac{Q(\Delta p)}{\pi R^2 \left(R_1 + \dfrac{d_0}{2} \right)} \tag{36}$$

For the motion resistance force of the medium in the hose, there is an obvious formula:

$$F(\dot{\varphi}) = \Delta p(\dot{\varphi}) \cdot \pi R^2 \tag{37}$$
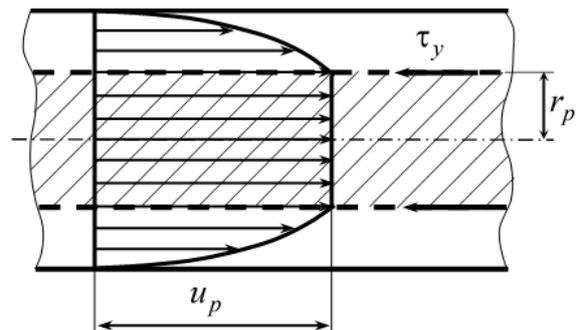
Fig. 9. Flow curve for Bingham fluid

Fig. 10. Bingham fluid flow diagram

Expression (36) cannot be solved analytically with relatively, that is, get a dependency $\Delta p = \Delta p(\dot\varphi)$. However, modern mathematical packages, in particular MathCAD, make it quite easy to get around these difficulties by using the interpolation of tabulated functions. Cubic spline interpolation was used in calculation studies. An important circumstance, in this case, is that the functions obtained in this way in the MathCAD environment can be used as traditional ones, in particular, they can be analytically differentiated.

This version of the algorithm implementation is convenient. On an equally uniformly spaced grid of pressure drop values (h_p – step by pressure drops) $\Delta p_i = \Delta p_{\min} + (i-1)h_p \ (i = \overline{1,N})$ by formula (36), we calculate the corresponding values of the angular velocity $\dot\varphi_i$. Now, considering $\dot\varphi_i$ as elements of the argument data vector (which should be put in order of ascending), and Δp_i as elements of the function value vector, by means of the built-in interpolation function, we build the required function $\Delta p(\dot\varphi)$. In the MathCAD package, the function *interp*(s,x,y,t) is used for cubic spline interpolation.

It is worth noting that the suggested approach can be easily transmissible to any real liquids with a nonlinear flow curve.

The nature of the dynamic processes in the pump significantly depends on the height that the mixture raises. The construction of a dynamic model in the form of the Lagrange equation with respect to the rotor rotation angle assumes finding a summarized force. It appeared to be convenient to take into account the effect of gravity forces of mixture particles as a component of the complete summarized force. The work of gravity forces of the mixture depends only on the difference in the heights of the hose ends. The shape of the hose between the extreme points does not matter, but the mass of the transferred mixture depends on the length of the hose (proportionally to its length). Therefore, when deriving the indicated expression, the hose can be assumed to be straight as shown in Figure 11.

Then the elementary vertical displacement of the mixture is determined from the proportion:

$$\frac{\delta z}{R_C \delta\varphi} = \frac{H_0}{l_0} \qquad (38)$$

where: $R_C = R - \dfrac{D}{2}$,
   $H_0 = H + 2R_C$ – total height of the mixture;

H – lift height of the outlet section end of the hose;

$2R_C$ – lift height of the mixture in the pump housing;

$l_0 = l_2 + \pi R_C$ – the length of the hose in which the mixture is being lifted;

l_2 – the length of the outlet section of the hose;

$\delta\varphi$ – summarized virtual movement of the rotor (φ – rotor rotation angle).

Now for the virtual work and the summarized force, we can write the formulas:

$$\delta A_{M_0} = -M_0 g \cdot \delta z = -M_0 g \frac{H_0}{l_0} R_C \cdot \delta\varphi = Q_{M_0}\delta\varphi$$

$$Q_{M_0} = -M_0 g \frac{H_0}{l_0} R_C \qquad (39)$$

where: $M_0 = \dfrac{\pi d^2}{4}\cdot l_0 \cdot \gamma$ – the mass of the mixture that rises;

   γ – the density of the mixture;

   g – acceleration of gravity.

To represent the moment of the hydraulic motor, the catalog data [25] was used. Characteristic dependences of the moment on the rotor speed for different hydraulic fluid consumption are presented in Figure 12. Consumption rates in liters per minute (L/min) are indicated next to each curve. The heavy line marks the curve used in the calculation studies of the experimental device model.

In Figure 13 it is shown the result of its restructuring dependency on the moment from the rotor angular velocity.

Dynamic model of the pump

It is convenient to represent the model in the form of the Lagrange equation of the second kind [27, 28], using the angle of rotor rotation as a generalized coordinate φ:

$$\frac{d}{dt}\frac{\partial T}{\partial \dot\varphi} - \frac{\partial T}{\partial \varphi} = Q_\varphi \qquad (40)$$

where: $T = T(\varphi,\dot\varphi)$ – kinetic energy of the system;
   $Q_\varphi = Q_\varphi(\varphi,\dot\varphi)$ – summarized force.

To obtain a summarized force, we compose an expression for the virtual work of forces acting on a mechanical system:

$$\delta A = \left(M_m(\dot\varphi) - M_k(\varphi) - F(\dot\varphi) \cdot R_C - M_0 g \cdot \frac{H_0}{l_0} \cdot R_C \right) \cdot \delta\varphi \quad (41)$$

where: $M_m(\dot\varphi)$ – moment of the hydraulic motor applied to the rotor;

$M_k(\varphi)$ – the total resistance moment on the rotor from the rolling of the rollers;

$-F(\dot\varphi) \cdot R_C$ – equivalent moment of resistance, due to the resistance forces to the movement of the mixture in the hose (see formula (37));

$-M_0 g \dfrac{H_0}{l_0} R_C$ – the equivalent moment of resistance due to the gravity forces of the particles of the mixture that rises (see formula (39)).
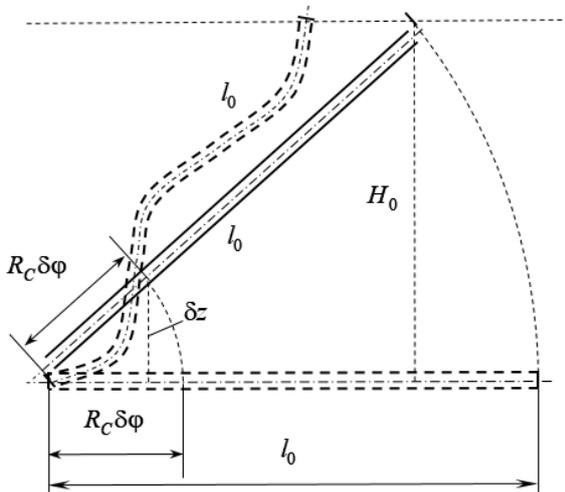
The expression in brackets of formula (41) is the summarized force:

$$Q_\varphi(\varphi,\dot\varphi) = M_m(\dot\varphi) - M_k(\varphi) - F(\dot\varphi) \cdot R_C - M_0 g \cdot \frac{H_0}{l_0} \cdot R_C \quad (42)$$

The kinetic energy of the rotor with rollers and the transported mixture:

$$T = T_0 + 2T_1 + 4T_2 + T_3 \quad (43)$$

where: $T_0 = \dfrac{1}{2}I\dot\varphi^2$ – kinetic energy of the rotor

I – the total inertia moment of the pump rotors (together with clips) and the motor);

$T_1 = \dfrac{1}{2}mv_{C_1}^2 + \dfrac{1}{2}I_1\omega_1^2$ – kinetic energy of the central roller ($v_{C_1} = \dot\varphi R_1$ – speed of the center of the central roller mass),

m – roller mass,

I_1 – axial moment of the roller inertia,

$\omega_1 = \dfrac{2v_{C_1}}{d_0}$ – angular velocity of the central roller);

$T_2 = \dfrac{1}{2}mv_{C_2}^2 + \dfrac{1}{2}I_1\omega_2^2$ – kinetic energy of the side roller ($v_{C_2} = \dot\varphi R_2$ – speed of the center of mass of the side roller,

$\omega_2 = \dfrac{2v_{C_2}}{d_0}$ – angular speed of the side roller);

$T_3 = \dfrac{1}{2}MR_C^2\dot\varphi^2$ – kinetic energy of the mixture ($M = \dfrac{\pi d^2}{4}l\gamma$ – mass of the mixture).

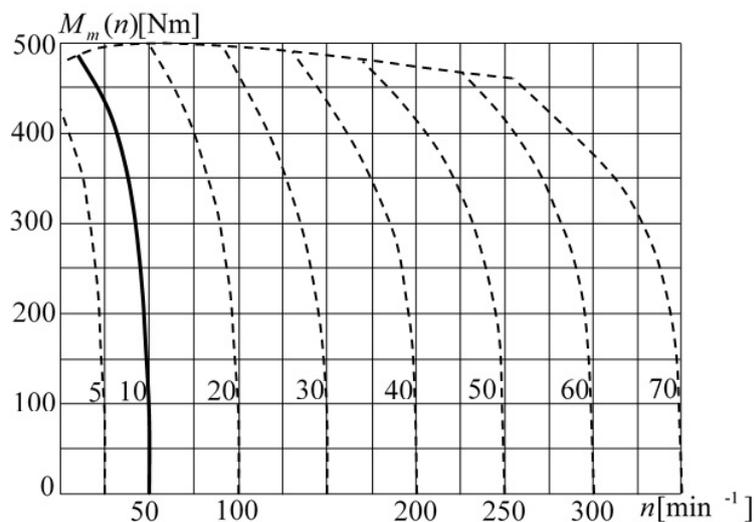From this perspective, formula (43) for the total kinetic energy of the system gives:

Fig. 11. Scheme for determining the generalized force for gravity forces when the mixture is lifted

Fig. 12. Dependence of the hydraulic motor on the rotational speed for various consumption of the operating fluid

$$T = \frac{1}{2}\left(I + 2\left(m + \frac{4I_1}{d_0^2}\right)\left(R_1^2 + 2R_2^2\right) + MR_C^2\right)\dot{\varphi}^2 = \frac{1}{2}I_e\dot{\varphi}^2 \quad (44)$$

where: I_e – equivalent moment of inertia:

$$I_e = I + 2\left(m + \frac{4I_1}{d_0^2}\right)\left(R_1^2 + 2R_2^2\right) + MR_C^2 \quad (45)$$

If the roller can be taken as a homogeneous cylinder, then $I_1 = \frac{1}{8}md_0^2$ formula (45) is simplified:

$$I_e = I + 3m\left(R_1^2 + 2R_2^2\right) + MR_C^2 \quad (46)$$

After performing the operations of the kinetic energy differentiation (44), the Lagrange equation (44), taking into account (46), takes the form:

$$I_e\ddot{\varphi} = Q_\varphi(\varphi, \dot{\varphi}) \quad (47)$$

This is the differential equation of rotor motion, which is necessary to integrate with the initial conditions: at $t = 0$, $\varphi = \varphi_0 = 0$, $\dot{\varphi} = \dot{\varphi}_0 = 0$.

The created multi-purpose arithmetic model of dynamic processes in a peristaltic pump underlying the algorithm implemented by means of the MathCAD mathematical package. Studies were conducted by means of the established program for the following values of the pump parameters: $d = 5$ cm; $h = 1.5$ cm; $D = 8$ cm; $R = 32$ cm; $R_1 = 23.7$ cm; $R_2 = 21.8$ cm; $d_0 = 10$ cm; $\alpha = 30°$; $\delta_1 = 3.5$ cm; $\delta_2 = 2.5$ cm; $G_1 = 500$ N; $G_2 = 250$ N;

$l_1 = 1$ m; $l_2 = 10$ m; $\mu = 4$ Pa · s; $g = 9.81$ m/s²; $m = 7.2$ kg; $I = 2.56$ kg· m²; $\gamma = 2300$ kg/m³.

In Figure 14 are shown the time dependences of the motion speed of the building mixture for three values of the height end of the outlet section of the hose: H = 0; H = 2.5; H = 5m. The following values of plastic viscosity and yield strength were used: $\mu_p = 10$ Pa · s, $\tau_y = 50$ Pa, .

A height increase in the lifting leads to a decrease in the average motion speed of the mixture, and the ripple frequency (the rotor speed decreases). In this case, the fluctuation amplitudes change insignificantly. There is a substantial impact of plastic viscosity and yield strength values on the mixture motion speed. With the same pump parameters for a Newtonian fluid with a dynamic-viscosity coefficient $\mu = 4$ Pa · s, the average motion speed occurs to be approximately twice as high [12].

When constructing diagrams in Figure 15 values of the yield strength were varied: $\tau_y = 0$; $\tau_y = 50$ Pa, $\tau_y = 100$ Pa.

Some initial model parameters have been changed: $\mu = 4$ Pa ; H = 0; l2 = 10m. Analysis of the graphs provides an opportunity to conclude that a significant change in the yield strength has little effect on the average velocity of the medium. The plastic viscosity of the medium has a much greater influence on the average velocity.

Convincing confirmation of the last statement is the diagrams in Figure 16. Curves 2 and 3, in contrast to the corresponding curves in Figure 16 were obtained for increased values of plastic viscosity $\mu = 6$ Pa, $\mu = 8$ Pa · s , which caused a significant decrease in the average motion speed of the medium.
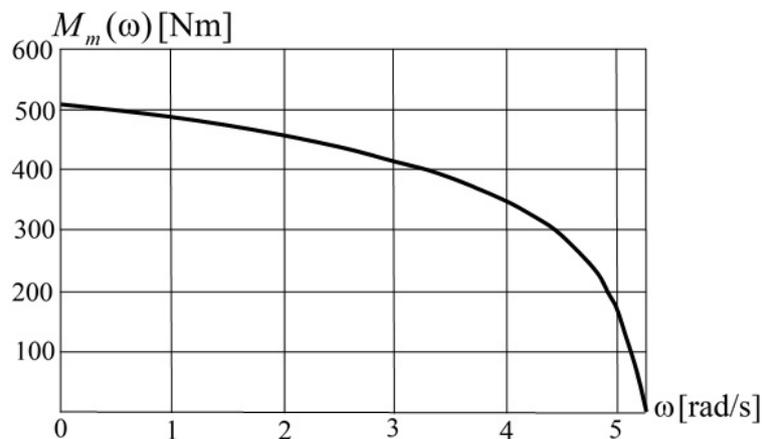

Fig. 13. Dependence of the moment of the hydraulic motor on the angular velocity of the rotor (consumption 10 L/min)

There was studied the effect of increasing the hydraulic motor power on the movement speed of the building mixture. The curve, which corresponds to the flow rate of the working fluid 20 L/min, was previously rebuilt into the dependence of the hydraulic motor moment on the rotor angular velocity as shown in Figure 17, since this was done at a flow rate 10 L/min as shown in Figure 13.

Diagrams of the dependences of the mixture motion speed versus time for this case are shown in Figure 18.

When constructing diagrams, the values of plastic viscosity $\mu = 2$ Pa · s; $\mu = 4$ Pa · s; $\mu = 6$ Pa · s), yield strength ($\tau_y = 0$, $\tau_y = 25$Pa, $\tau_y = 50$ Pa) were varied. For the mixture lifting height, the value was taken H = 5m ; other parameters

were taken as in the calculations when constructing the diagrams are shown in Figures 15, 16. The resulting diagrams show: that an increase in the power of the hydraulic motor leads to an increase in the average motion speed of the mixture (≈ 1 m/s; curve 1); an increase in plastic viscosity significantly reduces the average velocity of the mixture (curves 2, 3).

CONCLUSIONS

A mathematical model of dynamic processes in a peristaltic pump with a hydraulic drive has been created in the form of a differential equation with respect to the rotor rotation angle. The model contains the major geometrical, mass
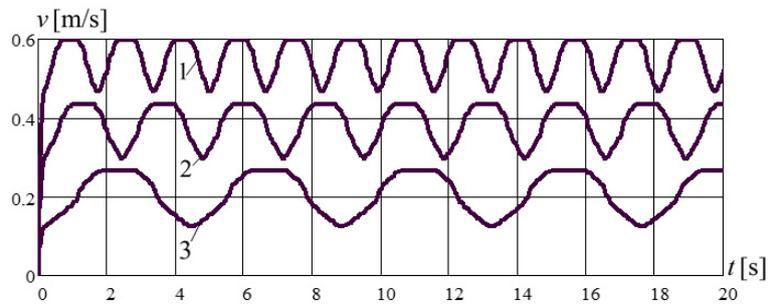

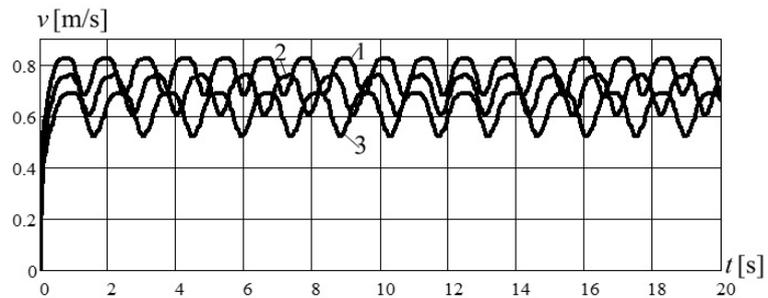**Fig. 14.** Mixture speed versus time (1 – H = 0; 2 – H = 2.5 m; 3 – H = 5m)

Fig. 15. Mixture speed versus time (1 – $\tau_y = 0$; 2 – $\tau_y =$ 50 Pa ; 3 – $\tau_y =$ 100 Pa)
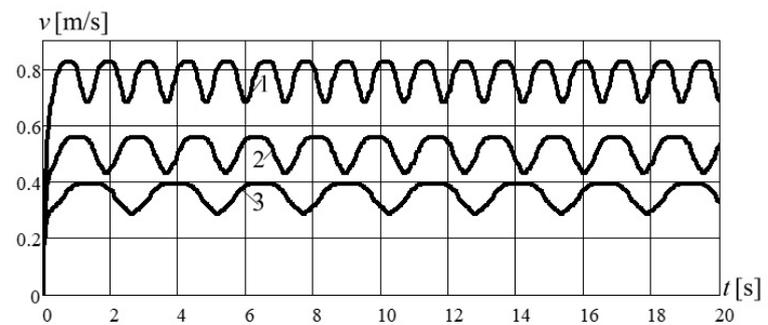
Fig. 16. Mixture speed versus time (1 – $\mu = 4$ Pa · s; $\tau_y = 4$ Pa · s; $\tau_y = 0$;
2 – $\mu = 6$ Pa · s; $\tau_y = 50$ Pa; 3 – $\mu = 8$ Pa · s; $\tau_y = 100$ Pa)
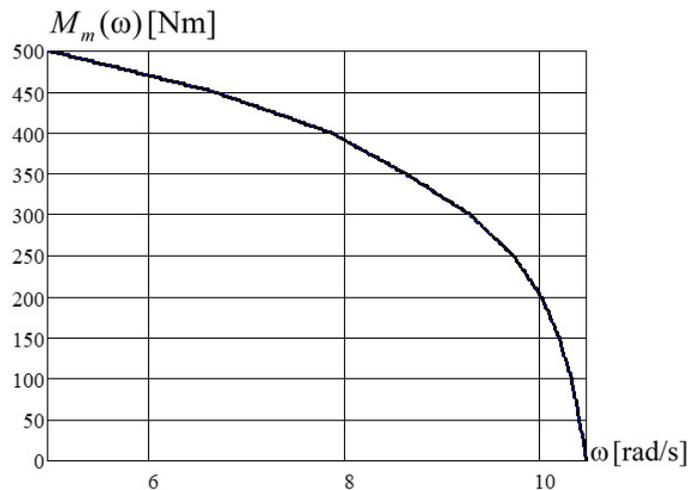
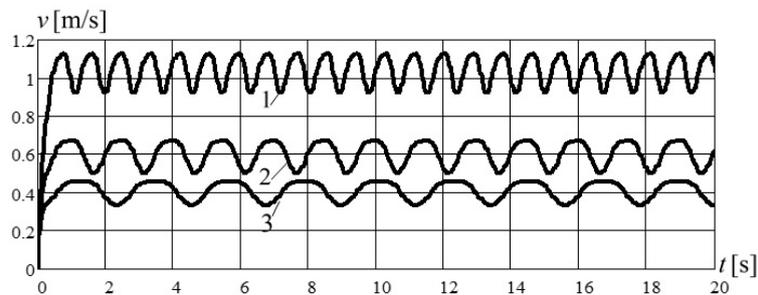**Fig. 17.** Dependence of the hydraulic motor moment on the angular velocity of the rotor (flow rate 20 L/min)

Fig. 18. Mixture speed versus time (1 – $\mu = 2$ Pa · s; $\tau_y = 0$; 2 – $\mu = 4$ Pa · s; $\tau_y = 25$ Pa; 3 – $\mu = 6$ Pa · s; $\tau_y = 50$Pa)

characteristics of the rotor, the dynamic characteristics of the hydraulic motor, the hose parameters, Bingham media.

A method has been developed for forming the resistance moment to the rotation of the pump rotor from the rollers that deform the hose; it was found that it is substantially different from the constant value on the interval of the turnover. This method is suggested for constructing the dependence of the pressure drop from the rotor angular velocity, which is necessary to determine the resistance force to the mixture movement by means of the Buckingham equation.

A nonlinear model of the force of resistance to the movement of the Bingham medium is proposed. The resistance force is the result of the action of the gravity forces of the mixture particles in the outlet part of the hose. Studies of dynamic processes have been performed by means of the created model. Important technological conformities of device functioning were established: the motion speed of the medium can have a significant variable component; the motion speed of the medium and the pump capacity increase with a

decrease in the length of the outlet hose and a decrease in the height of its rise; the plastic viscosity of the medium has a significant effect on the average velocity; a significant change in the yield strength has an effect on the speed insignificantly.

REFERENCES

1. Klespitz J., Kovács L. Peristaltic pumps – a review on working and control possibilities. IEEE 12th International Symposium on Applied Machine Intelligence and Informatics, Herl'any, Slovakia 2014, 191–194.

2. Patent application 'Universal hose pump'. Date: 26 September 2016; Number of priority application: UA 112585 C2.

3. Beyerle. Hose dosing pump. Maschinenmarkt 1978; 44: 868–870.

4. Kuskova M. Hydraulic characteristics of peristaltic pumps. The oil industry 2008; 1: 104–106.

5. Ivanchuk, Ya., Manzhilevskyy, O., Belzetskyi, R., Zamkovyi, O., Pavlovych, R. Modelling of piling technology by vibroimpact device with hydropulse drive. Scientific Horizons 2022; 25(1): 9–20. DOI: 10.48077/scihor.25(1).2022.9–20

6. Patent application 'Roller pump and peristaltic tubing with atrium'. Date 21 March 2008; Number of priority application: US 20090053084.

7. Iskovych–Lototsky R.D., Ivanchuk Y.V., Veselovsky Y.P. Simulation of working processes in the pyrolysis plant for waste recycling. Eastern–European Journal of Enterprise Technologies. Engineering technological systems 2016; 8(79): 11–20. DOI: 10.15587/1729–4061.2016.59419.

8. Dhananchezhiyan P., Hiremath S.S. Optimization of Multiple Micro Pumps to Maximize the Flow Rate and Minimize the Flow Pulsation. Procedia Technology 2016; 25: 1226–1233.

9. Ryzhakov A., Nikolenko I., Dreszer K. Selektion of discretely adjustable pump parameters for hydraulic drives of mobile eguipment. TEKA Kom. Mot. Energ. Roln.– OL. PAN 2009; 9: 267–276.

10. Rostislav D., Iskovych-Lototsky R., Yaroslav V., Ivanchuk Y., Veselovska N., Surtel W., Sundetov S. Automatic system for modeling vibro-impact unloading bulk cargo on vehicles, Proc. SPIE 10808, Photonics Applications in Astronomy, Communications, Industry, and High-Energy Physics Experiments 2018. DOI: 10.1117/12.2501526.

11. Henikl J., Kemmetmüller W., Bader M. Modeling, simulation and identification of a mobile concrete pump. Mathematical and Computer Modeling of Dynamical Sistems 2015; 21 (2): 180–201.

12. Bredel hose pumps. URL: https://www.watson-marlow.com/us-en/range/bredel/hose-pumps/ (accessed: 29.01.2020).

13. Rostislav D., Iskovych-Lototsky R., Ivanchuk Y., Veselovsky Y., Gromaszek K., Oralbekova A. Automatic system for modeling of working processes in pressure generators of hydraulic vibrating and vibro-impact machines, Proc. SPIE 10808, Photonics Applications in Astronomy, Communications, Industry, and High-Energy Physics Experiments 2018. DOI: 10.1117/12.2501532.

14. Peristaltic hose pumps for industry. PeriFlo. URL: http://www.periflo.com (accessed: 29.01.2020).

15. Shatokhin V., Granko B., Sobol V. Dynamic processes modeling in a peristaltic concrete pump with a hydraulic drive. Collection of scientific papers. Herald of the KhNADU 2020; 89: 15–25.

16. Aghakhani S., Pordanjani A., Karimipour A., Abdollahi A., Afrand M. Numerical investigation of heat transfer in a power-law non-Newtonian fluid in a C-shaped cavity with magnetic field effect using finite difference lattice Boltzmann method. Comput Fluids 2018; 176: 51–67.

17. Iskovich-Lototsky R., Kots I., Ivanchuk Y., Ivashko Y., Gromaszek K., Mussabekova A., Kalimoldayev M. Terms of the stability for the control valve of the hydraulic impulse drive of vibrating and vibro-impact machines. Electrotechnical review 2019; 4: 19–23. DOI: 10.15199/48.2019.04.04.

18. Yun N.T., Xiao P.Li, Qing H.Z., Bang C.W. Investigation on Nonlinear Dynamics Characteristics of Vibration Friction System Based on Vibration Pile Driver. Applied Mechanics and Materials 2016; 29–32: 2189–2193. DOI: 10.4028/www.scientific.net/AMM.29–32.

19. Voskresensky E.V. Asymptotic methods: theory and applications. Saransk: SVMO, 2001.

20. Guang L., Min W. Modeling and con-trolling of a flexible hydraulic manipulator. Journal of Central South University of Technology: Science & Technology of Mining and Metallurgy 2005; 12(5): 578–583.

21. Manzhilevskyy O. D. Analysis of hydraulic vibration drive machine for vibration abrasive processing. Electrotechnical review 2019; 1(4): 95 – 99. DOI: 10.15199/48.2019.04.16.

22. Matvienko O.V., Bazuev V.P., Sabylina N.R., Aseeva A.E., Surtaeva A.A. Study of the steady flow of a viscoplastic bituminous binder, described by the Shvedov Bingham model, in a cylindrical pipe. Sat. scientific works. Bulletin of the Tomsk State University of Architecture and Construction 2019; 21(3): 158–177. DOI: 10.31675/1607–1859–2019–21–3–158–177.

23. Faraji A., Razavi M., Fatouraee N. Linear peristaltic pump device design. Applied Mechanics and Materials. Advanced Materials & Sports Equipment Design 2014; 440: 199–203.

24. Walker S., Shelley M. Shape Optimization of Peristaltic Pumping. Journal of Computational Physics 2010; 229 (4): 1260–1291. DOI: 10.1016/j.jcp.2009. 10.030.

25. Sucharitha G., Streenadh S., Lakshminarayana P. Non-linear Peristaltic Flow of Pseudoplastic Fluid in an Asymmetric Channel with porous medium. International Journal of Engineering Science and Technology 2013; 5(1): 106–113.

26. Sevostianov I., Ivanchuk Y., Polishchuk O., Lutsyk V., Dobrovolska K., Smailova S., Wójcik W., Kalizhanova A. Development of the Scheme of the Installation for Mechanical Wastewater Treatment. Journal of Ecological Engineering 2021; 22(1): 20–28. DOI: 10.12911/22998993/128693.

27. Tesfaye O. Terefe, Hirpa G. Lemu, Addisu K/Mariam, Tadele B. Tuli. Kinematic Modeling and Analysis of a Walking Machine (Robot) Leg Mechanism on a Rough Terrain. Advances in Science and Technology Research Journal 2019; 13(3): 43–53. DOI: 10.12913/22998624/109792.

28. Kovalchuk R., Molkov Y., Lenkovskiy T., Grytsenko O., Krasinskyi V., Garbacz T. Drive System Parameters Influence on Run-Up Process of the Drilling Rig Pumping Unit. Advances in Science and Technology Research Journal 2018; 12(4): 199–206. DOI: 10.12913/22998624/100442.